ISSN 1674-1056
http://cpb.iphy.ac.cn
http://iopscience.iop.org/cpb
中国物理 B
Chinese Physics
中国物理 Chinese Physics B

Propagation properties of chirped Airy vortex beams with *x*-polarization through uniaxial crystals

Linyi Wang(王琳轶), Jianbin Zhang(张建彬), Liyan Feng(冯丽燕), Zihao Pang(庞子灏), Tianfen Zhong(钟甜芬), Dongmei Deng(邓冬梅)
Citation: Chin. Phys. B . 2018, 27(5): 054103. **doi:** 10.1088/1674-1056/27/5/054103

Journal homepage: http://cpb.iphy.ac.cn; http://iopscience.iop.org/cpb

What follows is a list of articles you may be interested in

Spatial chirp in Ti:sapphire multipass amplifier

Wenkai Li(黎文开), Jun Lu(陆俊), Yanyan Li(李妍妍), Xiaoyang Guo(郭晓杨), Fenxiang Wu(吴分翔), Linpeng Yu(於林鹏), Pengfei Wang(王朋飞), Yi Xu(许毅), Yuxin Leng(冷雨欣)
Chin. Phys. B . 2017, 26(3): 034206. **doi:** 10.1088/1674-1056/26/3/034206

High-energy femtosecond Yb-doped all-fiber monolithic chirped-pulse amplifier at repetition rate of 1 MHz

Zhi-Guo Lv(吕志国), Hao Teng(滕浩), Li-Na Wang(王立娜), Jun-Li Wang(王军利), Zhi-Yi Wei(魏志义)
Chin. Phys. B . 2016, 25(9): 094208. **doi:** 10.1088/1674-1056/25/9/094208

Nonparaxial propagation of Hermite-Laguerre-Gaussian beams in uniaxial crystal orthogonal to the optical axis

Xu Yi-Qing, Zhou Guo-Quan, Wang Xiao-Gang
Chin. Phys. B . 2013, 22(6): 064101. **doi:** 10.1088/1674-1056/22/6/064101

Switching the direction of spin accumulation in the spin Hall effect of light by adjusting the optical axis of an uniaxial crystal

Tang Ming, Zhou Xin-Xing, Xiao Zhi-Cheng, Luo Hai-Lu, Wen Shuang-Chun
Chin. Phys. B . 2013, 22(3): 034101. **doi:** 10.1088/1674-1056/22/3/034101

Characteristics of paraxial propagation of a super Lorentz–Gauss SLG_{01} mode in uniaxial crystal orthogonal to the optical axis

Zhou Guo-Quan
Chin. Phys. B . 2012, 21(5): 054104. **doi:** 10.1088/1674-1056/21/5/054104

Propagation properties of chirped Airy vortex beams with x-polarization through uniaxial crystals*

Linyi Wang(王琳昳), Jianbin Zhang(张建彬), Liyan Feng(冯丽燕), Zihao Pang(庞子灏), Tianfen Zhong(钟甜芬), and Dongmei Deng(邓冬梅)†

Guangdong Provincial Key Laboratory of Nanophotonic Functional Materials and Devices, South China Normal University, Guangzhou 510631, *China*

(Received 25 August 2017; revised manuscript received 2 January 2018; published online 26 April 2018)

The propagation dynamics of a chirped Airy vortex (CAiV) beam with x-polarization in uniaxial crystals orthogonal to the optical axis is studied analytically and numerically. The effect of the ratio of extraordinary and ordinary refractive indices, the chirp parameter, as well as the propagation distance is analyzed, which shows that the focused position of the CAiV beams can be controlled through changing the ratio of the extraordinary and ordinary refractive indices. In addition, with the propagation distance increasing, the asymmetry of the intensity and the angular momentum of the CAiV beam during propagation becomes much more visible. The variation of the chirp parameters can change the attenuation velocity of the vortex as well.

Keywords: chirp, uniaxial crystal, Airy vortex beams

PACS: 41.85.–p, 42.25.Bs, 42.65.Jx **DOI:** 10.1088/1674-1056/27/5/054103

1. Introduction

Ever since Airy wave packets, which are a solution of the Schrödinger equation in the background of quantum mechanics, were first discovered by Berry [1], research on these beams has advanced rapidly. The Airy beam can heal itself after being obscured by an obstacle.[2] What is more, these beams have a self-bending property as well as acceleration.[3] In practice, single solitons and soliton pairs can be produced during the interactions of similar Airy beams and nonlinear accelerating beams through Kerr and saturable nonlinear media.[4,5] In addition, the optical vortex is gradually noticed.[6] A vortex beam is a laser beam which contains a continuous spiral phase distribution.[7] Subsequently, the propagation dynamics of Airy vortex (AiV) beams, Airy Gaussian vortex (AiGV) beams and circular Airy vortex beams have been explored theoretically and experimentally.[8–10] In this paper, we add the chirp parameter on the basis of the AiV beams. Chirp is a phenomenon in which the signal changes frequently over time, the frequency spectrum will be widened before and after the pulse due to modulation.[11] The chirp has been applied for phase modulation when the beams propagate in different media.[12] The chirp parameter is used to describe this phenomenon.

Different from other isotropic medium, the uniaxial crystal is an anisotropic material that has unusual peculiarities.[13] Uniaxial crystal is always used in the design of optical devices because of its anisotropy impacting the polarization of light. In 2008, Deng *et al.* analyzed the propagation properties of hollow beams in uniaxial crystals, and they discovered that the symmetry of the beams was no longer maintained in the uniaxial crystals.[14] It is really interesting to analyze the propagation dynamics of light through anisotropic media in both applied and theoretical optics. The propagation properties of elliptical Gaussian beams, Airy–Hermite–Gaussian beams, Airy beams, Laguerre–Gaussian beams, Bessel–Gaussian beams and flattened-Gaussian beams in uniaxial crystals have been studied.[15–19] While the propagation of CAiV beams through uniaxial crystals has not been reported.

2. Analytical expression of chirped Airy vortex beams through uniaxial crystals

In the Cartesian coordinate system, the propagation axis is set as the z axis, and the x axis is taken to be the optical axis of the uniaxial crystal. The input plane is at $z = 0$ and the observation plane is taken to be z. The dielectric tensor of the uniaxial crystal is depicted as[20]

$$\varepsilon = \begin{pmatrix} n_{\mathrm{e}}^2 & 0 & 0 \\ 0 & n_{\mathrm{o}}^2 & 0 \\ 0 & 0 & n_{\mathrm{o}}^2 \end{pmatrix}, \tag{1}$$

where n_{e} and n_{o} are the extraordinary and the ordinary refractive indices of the uniaxial crystal, respectively.

The initial electric field distribution of the CAiV beam with x-polarization is

$$E_x(x,y,0) = Ai\left(\frac{x}{w_1}\right)Ai\left(\frac{y}{w_2}\right)\exp\left(\frac{ax}{w_1}+\frac{by}{w_2}\right) \times \exp\left(-\mathrm{i}C\frac{x^2+y^2}{w_0^2}\right)\left(\frac{x}{w_1}+\mathrm{i}\frac{y}{w_2}\right), \tag{2}$$

*Project supported by the National Natural Science Foundation of China (Grant Nos. 11775083 and 11374108), the National Training Program of Innovation and Entrepreneurship for Undergraduates, China, and Special Funds for the Cultivation of Guangdong College Students' Scientific and Technological Innovation, China (Grant No. pdjh2017b0137).

†Corresponding author. E-mail: dmdeng@263.net

© 2018 Chinese Physical Society and IOP Publishing Ltd

where w_0, w_1, and w_2 represent arbitrary transverse scales, $0 \le a < 1$ and $0 \le b < 1$ are the truncation factors making the CAiV beams have finite energy, C is the chirp parameter and $Ai(\cdot)$ is the Airy function. The total power of the finite energy CAiV beams with x-polarization reads

$$P = \iint_{-\infty}^{\infty} |E_x(x_0, y_0, 0)|^2 \, \mathrm{d}x_0 \, \mathrm{d}y_0. \tag{3}$$

The paraxial transmission of CAiV beams with x-polarization through uniaxial crystals can be described by

$$\begin{aligned} & E_x(x,y,z) \\ &= \frac{kn_\mathrm{o}}{2\pi \mathrm{i}z} \exp(\mathrm{i}kn_\mathrm{e}z) \iint_{-\infty}^{\infty} E_x(x_0, y_0, 0) \\ &\quad \times \exp\left\{ \frac{\mathrm{i}k}{2zn_\mathrm{e}} \left[n_\mathrm{o}^2 (x - x_0)^2 + n_\mathrm{e}^2 (y - y_0)^2 \right] \right\} \mathrm{d}x_0 \, \mathrm{d}y_0, \end{aligned} \tag{4}$$

where $k = 2\pi/\lambda$ is the wavenumber and λ is the wavelength of the incident light.

The analytical complex field distribution of CAiV beams with x-polarization through uniaxial crystals at distance z can be formulated as

$$E_x(x,y,z) = \frac{kn_\mathrm{o}}{2\mathrm{i}z} p_z \exp(F_1 + F_2)(P_1 + P_2 + P_3), \tag{5}$$

where

$$\begin{aligned} M &= \frac{\mathrm{i}C}{w_0^2} - \frac{\mathrm{i}kn_\mathrm{o}^2}{2zn_\mathrm{e}}, \quad N = \frac{\mathrm{i}C}{w_0^2} - \frac{\mathrm{i}kn_\mathrm{e}}{2z}, \\ p_z &= \frac{1}{\sqrt{MN}} \exp(\mathrm{i}kzn_\mathrm{e}) \exp\left[\frac{\mathrm{i}k}{2zn_\mathrm{e}} (n_\mathrm{o}^2 x^2 + n_\mathrm{e}^2 y^2) \right], \\ F_1 &= \frac{a^2}{4w_1^2 M} - \frac{\mathrm{i}kn_\mathrm{o}^2 xa}{2w_1 M z n_\mathrm{e}} + \frac{k^2 n_\mathrm{o}^4 x^2}{4Mz^2 n_\mathrm{e}^2} \\ &\quad + \frac{a}{8w_1^4 M^2} - \frac{\mathrm{i}kn_\mathrm{o}^2 x}{8w_1^3 M^2 z n_\mathrm{e}} + \frac{1}{96 w_1^6 M^3}, \\ F_2 &= \frac{b^2}{4w_2^2 N} - \frac{\mathrm{i}kn_\mathrm{e} yb}{2w_2 N z} + \frac{k^2 n_\mathrm{e}^2 y^2}{4Nz^2} \\ &\quad + \frac{b}{8w_2^4 N^2} - \frac{\mathrm{i}kn_\mathrm{e} y}{8w_2^3 N^2 z} + \frac{1}{96 w_2^6 N^3}, \\ P_1 &= Ai(G_1) Ai(G_2) \left[\left(\frac{1}{2w_1^4 M^2} - \frac{\mathrm{i}kn_\mathrm{o}^2 x}{2Mzn_\mathrm{e} w_1} \right) \right. \\ &\quad \left. + \mathrm{i} \left(\frac{1}{2w_2^4 N^2} - \frac{\mathrm{i}kn_\mathrm{e} y}{2Nzw_2} \right) \right], \\ P_2 &= \frac{1}{2w_1^2 M} Ai(G_2) \left[aAi(G_1) + Ai'(G_1) \right], \\ P_3 &= \frac{1}{2w_2^2 N} Ai(G_1) \left[aAi(G_2) + Ai'(G_2) \right], \\ G_1 &= \frac{1}{16w_1^4 M^2} + \frac{a}{2w_1^2 M} - \frac{\mathrm{i}kn_\mathrm{o}^2 x}{2w_1 M z^2 n_\mathrm{e}}, \\ G_2 &= \frac{1}{16w_2^4 N^2} + \frac{b}{2w_2^2 N} - \frac{\mathrm{i}kn_\mathrm{e} y}{2w_2 N z^2}. \end{aligned}$$

3. Numerical analysis and discussion of chirped Airy vortex beams

In order to illuminate the features of CAiV beams with x-polarization through uniaxial crystals more clearly, we investigate the trajectories with different ratios of n_e (the extraordinary index) and n_o (the ordinary index) as well as the intensity and the phase distributions at different distances with different chirp parameters.

Figure 1 describes the trajectory of CAiV beams with x-polarization in uniaxial crystals with $C = 0.001$, $n_\mathrm{o} = 2.616$, $a = b = 0.5$, $w_1 = w_2 = 10^{-4}$ mm. A 633 nm laser is used. Figures 1(a)–1(c) show the propagation dynamics when n_o is not equal to n_e. Figure 1(d) presents the propagation dynamics of the CAiV beams when $n_\mathrm{o} = n_\mathrm{e} = 2.616$ (isotropic medium). The figures shows that the wave is discontinuous when the CAiV beams propagate through the uniaxial crystal, while it is constant when propagating through the isotropic medium. Even more evidently, the ratio of n_e and n_o affects the continuity and the bending degree of the CAiV beams during the propagation. When the ratio of n_e and n_o is increasing, the bending degree of the CAiV beams, which is caused by the self-accelerated characteristics of the Airy packet, is decreasing. What is more, when the ratio of n_e and n_o is increasing, the focused position of the CAiV beams is approaching the origin.

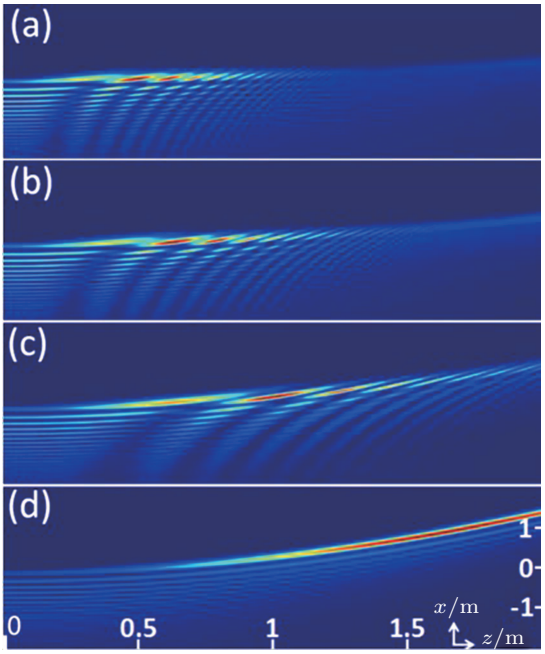


Fig. 1. (color online) Propagation dynamics of CAiV beams as a function of distance when (a) $n_\mathrm{e} = 1.8n_\mathrm{o}$, (b) $n_\mathrm{e} = 1.5n_\mathrm{o}$, (c) $n_\mathrm{e} = 1.2n_\mathrm{o}$, (d) $n_\mathrm{e} = n_\mathrm{o} = 2.616$.

Figure 2 presents the maximum intensity of the CAiV beams with x-polarization as a function of the propagation distance, which shows that the maximum intensity of the CAiV beams firstly increases as the distance increases due to the

optical vortex. Then the maximum intensity of the CAiV beams decreases during further propagation but is not decreasing monotonously due to the anisotropic effect of the uniaxial crystal.

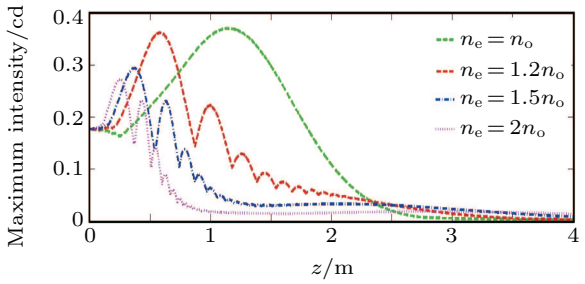


Fig. 2. (color online) The maximum intensity of the CAiV beams as a function of propagation distance.

To discuss the effect of the chirp parameter C, we take $a = b = 0.01$, $n_o = 2.616$, $n_e = 3.1392$, $w_1 = w_2 = 10^{-4}$ mm with different chirp parameters. In Figs. 3(a1)–3(a6) with $C = -1$, we can find that, as the distribution factor increases, the energy will reverse, yet when the absolute value of C approaches 0, it cannot happen. Evidently, as the absolute value of the chirp parameter increases, if we change the sign of the chirp parameter, there will be an energy reversal. The reason is that the optical phase is modulated by the chirp parameter, which is shown in Fig. 4.

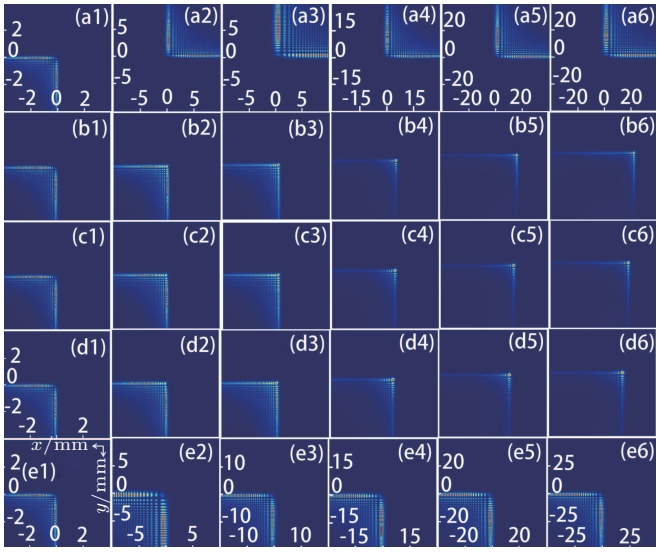


Fig. 3. (color online) Intensity profiles of CAiV beams with (a1)–(a6) $C = -1$, (b1)–(b6) $C = -0.01$, (c1)–(c6) $C = 0$, (d1)–(d6) $C = 0.01$, and (e1)–(e6) $C = 1$ at the planes of (a1)–(e1) $z = 0$, (a2)–(e2) $z = 0.496$ m, (a3)–(e3) $z = 0.6944$ m, (a4)–(e4) $z = 1.24$ m, (a5)–(e5) $z = 1.6864$ m, and (a6)–(e6) $z = 1.8848$ m.

To further analyze the influences of the chirp parameters and the distribution factors, we plot Fig. 5 with $a = b = 0.01$, $n_o = 2.616$, $n_e = 3.1392$, and $w_1 = w_2 = 10^{-4}$ mm, which depicts the intensity distributions of the CAiV beams with x-polarization through uniaxial crystals at different distances with different chirp parameters. From these figures, we can see that the intensity first distributes in the side lobes because of the vortex and, as the CAiV beams propagate, the intensity distributions in the main lobes are strengthened and those in the side lobes are weakened, the reason for this is that the acceleration of the vortex is much higher than that of the main lobe. Meanwhile, compared with the traditional vortex modulated by the dressing nonlinear phase in an atomic ensemble whose characteristics can be controlled by the laser intensities, nonlinear dispersion, atomic density, detunings and intensities of the related generating fields,[21,22] the chirp parameters will affect the velocity of the vortex in the uniaxial crystals. When the chirp factor increases, the velocity of the vortex decreases. Interestingly, we can also find that when the chirp parameter approaches 0, the intensity profile will not keep symmetrical with the propagation distance increasing.

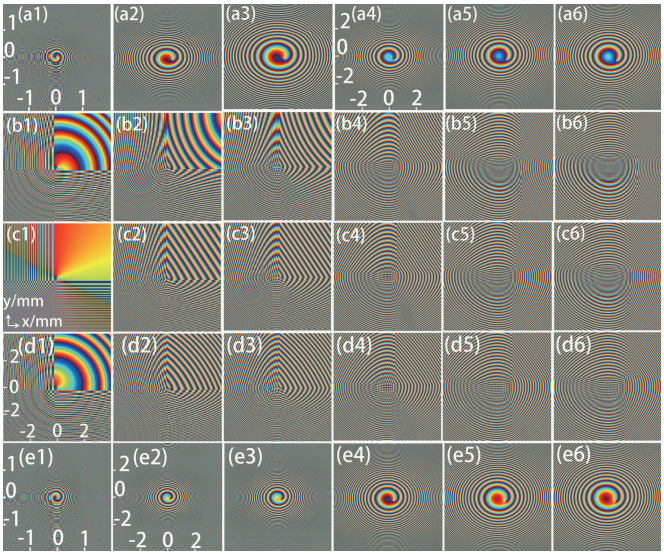


Fig. 4. (color online) The phase distribution of the CAiV beams. All the parameters are the same as those in Fig. 3.

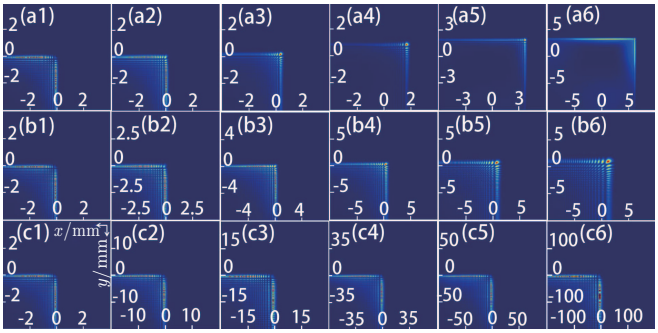


Fig. 5. (color online) Intensity profiles of CAiV beams with (a1)–(a6) $C = 0.01$, (b1)–(b6) $C = 0.1$, (c1)–(c6) $C = 1$ at the planes of (a1)–(c1) $z = 0$ m, (a2)–(c2) $z = 0.5$ m, (a3)–(c3) $z = 1$ m, (a4)–(c4) $z = 2$ m, (a5)–(c5) $z = 3$ m, and (a6)–(c6) $z = 4$ m.

Figure 6 shows the phase distribution of CAiV beams with different chirp parameters and propagation distances. It is easy to see that the influence of the chirp parameters on the

phase distributions is large, especially when the chirp parameters and the propagation distances are increasing.

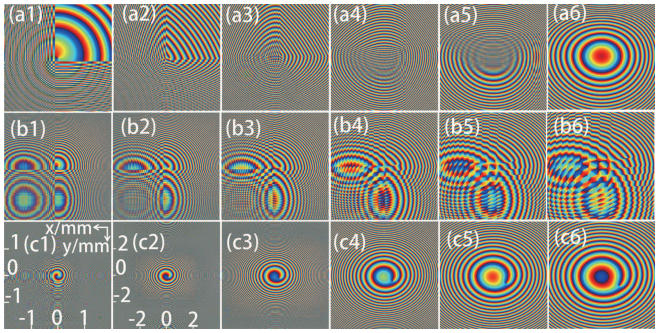


Fig. 6. (color online) The phase distribution of the CAiV beams. All the parameters are the same as those in Fig. 5.

4. Poynting vector of the chirped Airy vortex beams

To analyze the propagation properties of the CAiV beams with x-polarization through uniaxial crystals, we calculate the Poynting vector. We use the Poynting vector to illustrate the propagation dynamics of the CAiV beams. The Poyting vector can be expressed as $\boldsymbol{S} = \frac{c}{4\pi}\langle \boldsymbol{E} \times \boldsymbol{B} \rangle$, where c is the speed of light in vacuum, $\boldsymbol{E}$ is the electric field, and $\boldsymbol{B}$ is the magnetic induction vector. The time-averaged Poynting vector can be expressed as[23,24]

$$\langle \boldsymbol{S} \rangle = \frac{c}{4\pi}\langle \boldsymbol{E} \times \boldsymbol{B} \rangle. \tag{6}$$

It is known by the Maxwell equation that

$$\boldsymbol{B} = \frac{-\mathrm{i}}{\omega}\nabla \times \boldsymbol{E} = \frac{-\mathrm{i}}{\omega}\left(\frac{\partial E_x}{\partial z}\boldsymbol{e}_y - \frac{\partial E_x}{\partial y}\boldsymbol{e}_z\right). \tag{7}$$

By substituting Eq. (7) into Eq. (6), we have

$$\boldsymbol{S} = \frac{-\mathrm{i}c}{4\pi\omega}\left[E_x\left(\frac{\partial E_x}{\partial y}\right)\boldsymbol{e}_y + E_x\left(\frac{\partial E_x}{\partial z}\right)\boldsymbol{e}_z\right]. \tag{8}$$

Figure 7 presents the Poynting vectors of CAiV beams with different chirp parameters and propagating distances through the uniaxial crystals. The magnitude and the direction of the energy flow are shown clearly by the size and the direction of the arrows, respectively. It is discovered that the initial vortex is at the center. As the propagation distance increases, the vortex is moving away from the center and the vortex is gradually weakened in Fig. 7. Lastly, the energy flow is only along the y axis.

On the other hand, with different chirp parameters, the distributions of the vortex are different. It is clearly seen that, as the chirp parameter increases, the attenuation velocity of the vortex becomes slower.

The angular momentum plays an important part in electromagnetism.[25] The time-averaged angular momentum density can be written as[26]

$$\langle \boldsymbol{J} \rangle = \boldsymbol{r} \times \langle \boldsymbol{E} \times \boldsymbol{B} \rangle = \frac{4\pi}{c}\boldsymbol{r} \times \boldsymbol{S}. \tag{9}$$

By substituting Eq. (8) into Eq. (9), we have

$$\begin{aligned}\boldsymbol{J} &= -\frac{i}{\omega}[(yS_z - zS_y)\boldsymbol{e}_x - xS_z\boldsymbol{e}_y + xS_y\boldsymbol{e}_z] \\ &= -\frac{i}{\omega}E_x\left\{\left[y\left(\frac{\partial E_x}{\partial z}\right) - z\left(\frac{\partial E_x}{\partial y}\right)\right]\boldsymbol{e}_x \right. \\ &\quad \left. -x\left(\frac{\partial E_x}{\partial z}\right)\boldsymbol{e}_y + x\left(\frac{\partial E_x}{\partial y}\right)\boldsymbol{e}_z\right\}. \end{aligned} \tag{10}$$

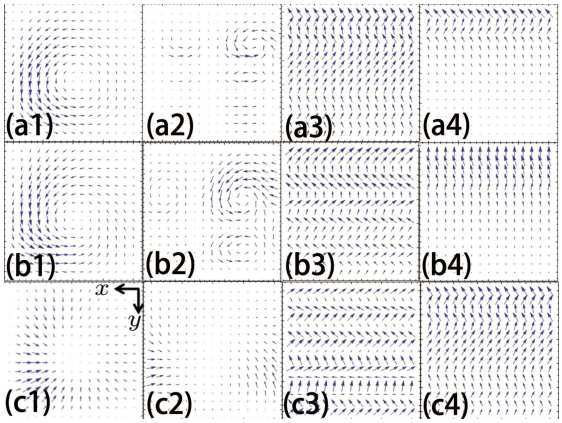


Fig. 7. (color online) Energy flow of CAiV beams with (a1)–(a4) $C = 0.01$, (b1)–(b4) $C = 0.1$, (c1)–(c4) $C = 1$ at the planes of (a1)–(c1) $z = 0.0496$ m, (a2)–(c2) $z = 0.0992$ m, (a3)–(c3) $z = 0.248$ m, and (a4)–(c4) $z = 0.3968$ m.

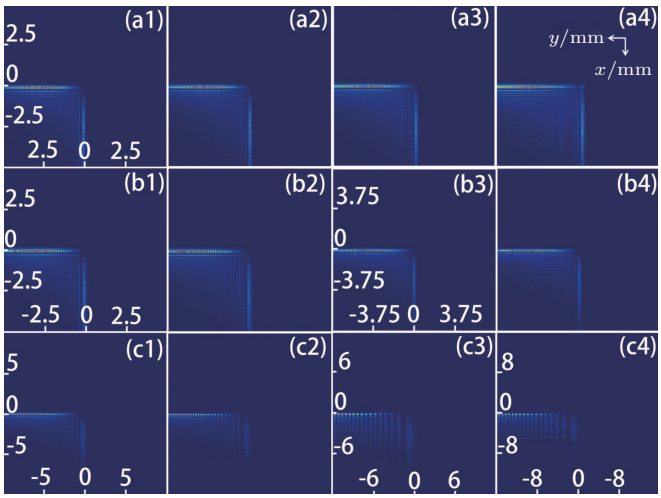


Fig. 8. (color online) Angular momentum of CAiV beams with (a1)–(a4) $C = 0.01$, (b1)–(b4) $C = 0.1$, (c1)–(c4) $C = 1$ at the planes of (a1)–(c1) $z = 0.0496$ m, (a2)–(c2) $z = 0.0992$ m, (a3)–(c3) $z = 0.248$ m, and (a4)–(c4) $z = 0.3968$ m.

Figure 8 shows the angular momentum of CAiV beams at different distances and with different chirp parameters. It is obvious that the initial angular momentum density flow is in the transverse direction, which is stronger than that in the longitudinal direction. With the propagating distance increasing, the angular momentum density flow in the transverse direction becomes much stronger and approaches the negative direction of the x axis, and that in the longitudinal direction is weaker and even approaches 0. Evidently, when C is increasing, the

asymmetry of the angular momentum of the CAiV beams is more obvious. It also proves that the anisotropy of uniaxial crystals can break the symmetry of propagating CAiV beams.

5. Conclusion

We investigate the propagation properties of CAiV beams with x-polarization in uniaxial crystals. It is clear that the focused position can be controlled by changing the ratio of n_e and n_o. In addition, the results show that the continuity and the self-acceleration effect of the CAiV beams become weaker as the proportion increases. From the intensity and the phase distributions of the CAiV beams, we find that the variation of the chirp parameters can affect the attenuation velocity of the vortex and control the intensity distribution. What is more, by changing the sign of the chirp parameter, we can control the intensity distribution of the CAiV beams. Lastly, we discuss the energy flow and the angular momentum of the CAiV beams through uniaxial crystals with different chirp parameters and discover that, when the distribution factor or the chirp parameter is increasing, the asymmetry of the angular momentum is more probable.

References

[1] Berry M V and Balazs N L 1979 *American Journal of Physics* **47** 264
[2] Broky J, Siviloglou G A, Dogariu A and Christodoulides D N 2008 *Opt. Express* **16** 12880
[3] Sivilogou G A, Broky J, Dogariu A and Christodoulides D N 2007 *Phys. Rev. Lett.* **99** 213901
[4] Zhang Y Q, Belić M R, Wu Z k, Zheng H B, Lu K Q, Li Y Y and Zhang Y P 2013 *Opt. Lett.* **38** 4585
[5] Zhang Y Q, Belić M R, Zheng H B, Chen H X, Li C B, Li Y Y and Zhang Y P 2014 *Opt. Express* **22** 7160
[6] Verbeeck J, Tian H and Schattschneider P 2010 *Nature* **467** 301
[7] Lu X H, Huang H Q, Zhao C L, Wang J F and Chen H 2008 *Laser and Optoelectronics Progress* **01** 50
[8] Huang J Y, Liang Z J, Deng F, Yu W H, Zhao R H, Chen B, Yang X B and Deng D M 2015 *J. Opt. Soc. Am. A* **32** 2104
[9] Chen B, Chen C D, Peng X and Deng D M 2015 *J. Opt. Soc. Am. B* **32** 173
[10] Zhang Y Q, Liu X, Belić M R, Zhong W P, Wen F and Zhang Y P 2015 *Opt. Lett.* **40** 3786
[11] Dorsch R G, Lohmann A W, Bitran Y, Mendlovic D and Ozaktas H M 1994 *Appl. Opt.* **33** 7599
[12] Matsui Y, Mahgerefteh D, Zheng X Y, Liao C, Fan Z F, McCallion K and Tayebati P 2006 *IEEE Photonics Telechnology Letters* **18** 385
[13] Zhang W L, Zhang T R, Li Y T, Huang Y C, Song H Y and Bao J Q 2011 *Acta Optica Sinica* **31** 0826001
[14] Deng D, Yu H, Xu S, Shao J and Fan Z 2008 *Opt. Commun.* **281** 202
[15] Huang Y C, Zhang T R, Chen S H, Song H Y, Li Y T and Zhang W L 2011 *Acta Phys. Sin.* **60** 074212 (in Chinese)
[16] Yu J, Xiao S, Yao L, Liu S and Li J 2017 *J. Mod. Opt.* **64** 616
[17] Zhou G Q, Chen R P and Chu X X 2012 *Opt. Express* **20** 2196
[18] Ciattoni A, Palma C and Cincotti G 2002 *J. Opt. Soc. Am. A* **19** 1680
[19] Luo S R and Lv B D 2003 *Acta. Phys. Sin.* **52** 3061 (in Chinese)
[20] Deng D M, Chen C D, Zhao X and Li H G 2013 *Appl. Phys. B* **110** 433
[21] Zhang Y P, Nie Z Q, Zhao Y, Li C B, Wang R M, Si J H and Xiao M 2010 *Opt. Express* **18** 10963
[22] Zhang D, Liu X, Yang L M, Li X H, Zhang Z H and Zhang Y P 2017 *Opt. Lett.* **42** 3097
[23] Allen L and Padgett M J 2000 *Opt. Commun.* **184** 67
[24] Padgett M J and Allen L 1995 *Opt. Commun.* **121** 36
[25] Barnett S M 2002 *J. Opt. B* **4** S7
[26] Garces-Chavez V, Arlt J, Dholakia K and Volke-Sepulveda K 2002 *J. Opt. B* **4** S82